

The Nonlinear Kinetic Sunyaev-Zeldovich Effect

Chung-Pei Ma¹ and J. N. Fry²

¹Department of Physics & Astronomy, University of Pennsylvania, Philadelphia PA 19104; cpma@physics.upenn.edu

²Department of Physics, University of Florida, Gainesville FL 32611-8440; fry@phys.ufl.edu

We derive fully nonlinear expressions for temperature fluctuations from the kinetic Sunyaev-Zeldovich effect, the scattering of cosmic microwave background (CMB) photons off hot electrons in bulk motion. Our result reproduces the Ostriker-Vishniac effect to second order in perturbation theory but contains important nonlinear contributions from the electron velocities and densities that were neglected previously. We use the recently developed halo model for nonlinear gravitational clustering to compute the nonlinear CMB power spectrum, which dominates the primary anisotropy on small angular scales.

PACS numbers: 98.80.Es, 98.65.Dx, 98.70.Vc

Introduction.—Scattering of cosmic microwave background (CMB) photons from hot electrons in galaxies and clusters changes the apparent brightness of the CMB, inducing anisotropies in the observed temperature, the Sunyaev-Zeldovich (SZ) effect [1]. The kinetic SZ effect due to scattering off ionized matter in bulk peculiar motion can be separated from the thermal SZ effect due to electron pressure by its different dependence on photon frequency; in particular, the kinetic effect dominates at frequencies around 218 GHz where the thermal effect vanishes. These foreground contributions are overwhelmed by primary anisotropies for spherical harmonic index ℓ smaller than a few thousand but can dominate at higher ℓ .

The kinetic SZ effect vanishes at leading order in perturbation theory for small inhomogeneities [2,3] (see below). At second order, however, it generates temperature fluctuations on arcminute angular scales, as first pointed out by Ostriker and Vishniac (OV) [4,5]. The OV power spectrum has since been studied in some detail [6–11]. In this letter we investigate analytically the fully nonlinear effect, which has not been much studied previously but is potentially important because reionized material in the low-redshift universe mostly resides in collapsed, high density objects. Our analytical approach complements recent kinetic SZ studies with hydrodynamical simulations [12] and helps to provide physical insight into why simulation results differ greatly on small scales.

The fractional temperature distortion due to the kinetic SZ effect along the line-of-sight unit vector $\hat{\gamma}$ is

$$\frac{\Delta T}{T}(\hat{\gamma}) = \int dl e^{-\tau} n_e \sigma_T \hat{\gamma} \cdot \mathbf{v} = \int dl e^{-\tau} \bar{n}_e \sigma_T \hat{\gamma} \cdot \mathbf{q}, \quad (1)$$

where τ is the optical depth from the observer to a scatterer of peculiar velocity \mathbf{v} and σ_T is the Thomson cross section. The electron density is $n_e = \bar{n}_e(1 + \delta)$, where δ is the density contrast, $\bar{n}_e = X_e \Omega_b \rho_c (1 + z)^3 / m_p$ is the proper mean electron density at redshift z , X_e is the ionization fraction, Ω_b is today's baryon density parameter, ρ_c is the critical density, and m_p is the proton mass.

The density-weighted peculiar velocity \mathbf{q} and its Fourier transform $\tilde{\mathbf{q}}$ are $\mathbf{q}(\mathbf{x}) = \mathbf{v}(1 + \delta)$ and

$$\tilde{\mathbf{q}}(\mathbf{k}) = \tilde{\mathbf{v}}(\mathbf{k}) + \int \frac{d^3 k'}{(2\pi)^3} \tilde{\mathbf{v}}(\mathbf{k}') \tilde{\delta}(\mathbf{k} - \mathbf{k}'), \quad (2)$$

where $\tilde{\delta}$ and $\tilde{\mathbf{v}}$ are the Fourier transforms of δ and \mathbf{v} . The angular two-point correlation function of the CMB anisotropy $C(\theta)$ is

$$C(\theta) = \left\langle \frac{\Delta T}{T}(\hat{\mathbf{n}}_1) \frac{\Delta T}{T}(\hat{\mathbf{n}}_2) \right\rangle = \sum_{\ell=0}^{\infty} \frac{(2\ell + 1)}{4\pi} C_{\ell} \mathcal{P}_{\ell}, \quad (3)$$

where C_{ℓ} is the angular power spectrum, and $\mathcal{P}_{\ell}(\cos \theta) = \mathcal{P}_{\ell}(\hat{\mathbf{n}}_1 \cdot \hat{\mathbf{n}}_2)$ are the Legendre polynomials. For $\ell \gg 1$, the C_{ℓ} can be calculated by projecting the 3-d power spectrum in the small-angle approximation [7,10,13]. For the kinetic SZ effect, we find

$$C_{\ell} = \frac{\bar{n}_{e,0}^2 \sigma_T^2}{H_0^2} \int \frac{dx}{x^2} (1 + z)^4 e^{-2\tau} P_{q_{\gamma}} \left(\frac{\ell}{x}, z \right), \quad (4)$$

where $P_{q_{\gamma}}(k, z)$ is the power spectrum of the line-of-sight component $\hat{\gamma} \cdot \tilde{\mathbf{q}}$, and x denotes comoving distance; in zero curvature models, $dx = H_0^{-1} dz / \sqrt{\Omega_m (1 + z)^3 + \Omega_{\Lambda}}$.

The key quantity for us to compute is therefore $P_{q_{\gamma}}$ in the fully nonlinear theory. Before deriving it, we first note an important feature of the kinetic SZ effect: Due to (near-)cancellations in the radial projection in Eq. (4), only modes with orientation $\hat{\mathbf{k}}$ perpendicular to $\hat{\gamma}$ contribute to the integrated effect [3,10]. This implies that the density-weighted velocity along the line of sight obeys $\hat{\gamma} \cdot \tilde{\mathbf{q}} = \hat{\gamma} \cdot (\tilde{\mathbf{q}}_{\parallel} + \tilde{\mathbf{q}}_{\perp}) \approx \hat{\gamma} \cdot \tilde{\mathbf{q}}_{\perp}$, where we decompose $\tilde{\mathbf{q}}$ into a longitudinal component $\tilde{\mathbf{q}}_{\parallel} = \hat{\mathbf{k}}(\tilde{\mathbf{q}} \cdot \hat{\mathbf{k}})$ and a transverse component $\tilde{\mathbf{q}}_{\perp} = \tilde{\mathbf{q}} - \hat{\mathbf{k}}(\tilde{\mathbf{q}} \cdot \hat{\mathbf{k}})$ relative to $\hat{\mathbf{k}}$. Defining

$$\begin{aligned} \langle \tilde{\mathbf{q}}_{\perp}(\mathbf{k}) \cdot \tilde{\mathbf{q}}_{\perp}(\mathbf{k}') \rangle &= (2\pi)^3 \delta_D(\mathbf{k} + \mathbf{k}') P_{q_{\perp}}(k), \\ \langle \tilde{\mathbf{q}}_{\parallel}(\mathbf{k}) \cdot \tilde{\mathbf{q}}_{\parallel}(\mathbf{k}') \rangle &= (2\pi)^3 \delta_D(\mathbf{k} + \mathbf{k}') P_{q_{\parallel}}(k), \end{aligned} \quad (5)$$

we then have the simple relation $P_{q_{\gamma}} \approx \frac{1}{2} P_{q_{\perp}}$. Although q_{\parallel} does not contribute to the kinetic SZ effect directly,

we will keep track of this component because it has a simple physical meaning: the equation of continuity $a\dot{\delta} + \nabla \cdot [(1 + \delta)\mathbf{v}] = 0$ becomes $\tilde{\mathbf{q}}_{\parallel}(\mathbf{k}, t) = (i a \mathbf{k}/k^2) \dot{\delta}(\mathbf{k}, t)$ in the Fourier domain; q_{\parallel} is therefore proportional to the time derivative of the density field δ .

Our task now is to compute $P_{q_{\perp}}$ and $P_{q_{\parallel}}$. To linear order, we have $\tilde{\mathbf{q}} = \tilde{\mathbf{v}} \propto \hat{\mathbf{k}}$, so $\tilde{\mathbf{q}}_{\perp} = 0$ and the linear kinetic SZ effect is negligibly small [3]. In the nonlinear regime where $\delta > 1$, the second term of $\tilde{\mathbf{q}}$ in Eq. (2) dominates, so we will focus on this term from this point on. The power spectrum for $\tilde{\mathbf{q}}$ will then be the fourth moment of two δ and two \mathbf{v} fields. In general, the fourth moment for quantities with zero mean has contributions from second moments of all possible pairs plus an irreducible or connected fourth moment: $\langle ABCD \rangle = \langle AB \rangle \langle CD \rangle + \langle AC \rangle \langle BD \rangle + \langle AD \rangle \langle BC \rangle + \langle ABCD \rangle_c$. Using

$$\begin{aligned} \langle \tilde{\delta}(\mathbf{k}_a) \tilde{\delta}(\mathbf{k}_b) \rangle &= (2\pi)^3 \delta_D(\mathbf{k}_a + \mathbf{k}_b) P_{\delta\delta}(k_a) \\ \langle \tilde{\mathbf{v}}^i(\mathbf{k}_a) \tilde{\mathbf{v}}^j(\mathbf{k}_b) \rangle &= (2\pi)^3 \delta_D(\mathbf{k}_a + \mathbf{k}_b) \hat{\mathbf{k}}_a^i \hat{\mathbf{k}}_b^j P_{vv}(k_a) \\ \langle \tilde{\delta}(\mathbf{k}_a) \tilde{\mathbf{v}}^i(\mathbf{k}_b) \rangle &= (2\pi)^3 \delta_D(\mathbf{k}_a + \mathbf{k}_b) \hat{\mathbf{k}}_b^i P_{\delta v}(k_a) \\ \langle \tilde{\delta}(\mathbf{k}_a) \tilde{\delta}(\mathbf{k}_b) \tilde{\mathbf{v}}^i(\mathbf{k}_c) \tilde{\mathbf{v}}^j(\mathbf{k}_d) \rangle_c &= (2\pi)^3 \delta_D(\Sigma \mathbf{k}_{\alpha}) \hat{\mathbf{k}}_c^i \hat{\mathbf{k}}_d^j P_{\delta\delta vv}(\mathbf{k}_a, \mathbf{k}_b, \mathbf{k}_c, \mathbf{k}_d). \end{aligned} \quad (6)$$

we can then write the power spectrum for $\tilde{q}_i \tilde{q}_j$ as

$$\begin{aligned} P_{qq}^{ij}(k) &= \int \frac{d^3 k'}{(2\pi)^3} \frac{d^3 k''}{(2\pi)^3} \{ (2\pi)^3 \delta_D(\mathbf{k} - \mathbf{k}' - \mathbf{k}'') \\ &\quad \times [\hat{\mathbf{k}}^{i'j'} P_{vv}(k') P_{\delta\delta}(k'') + \hat{\mathbf{k}}^{i'j'} \hat{\mathbf{k}}^{i''j''} P_{\delta v}(k') P_{\delta v}(k'')] \\ &\quad + \hat{\mathbf{k}}^{i'j'} \hat{\mathbf{k}}^{i''j''} P_{\delta\delta vv}(\mathbf{k} - \mathbf{k}', -\mathbf{k} - \mathbf{k}'', \mathbf{k}', \mathbf{k}'') \}. \end{aligned} \quad (7)$$

From $P_{q_{\perp}} = 2P_{q_{\gamma}} = 2\tilde{\gamma}^i \tilde{\gamma}^j P_{qq}^{ij}$ and $P_{q_{\parallel}} = \hat{\mathbf{k}}^i \hat{\mathbf{k}}^j P_{qq}^{ij}$, we obtain the main equation in this letter:

$$\begin{aligned} P_{q_{\perp}}(k) &= \int \frac{d^3 k'}{(2\pi)^3} \left[(1 - \mu'^2) P_{\delta\delta}(|\mathbf{k} - \mathbf{k}'|) P_{vv}(k') \right. \\ &\quad \left. - \frac{(1 - \mu'^2) k'}{|\mathbf{k} - \mathbf{k}'|} P_{\delta v}(|\mathbf{k} - \mathbf{k}'|) P_{\delta v}(k') \right] \\ &+ \int \frac{d^3 k'}{(2\pi)^3} \frac{d^3 k''}{(2\pi)^3} \sqrt{1 - \mu'^2} \sqrt{1 - \mu''^2} \cos(\phi' - \phi'') P_{\delta\delta vv}, \\ P_{q_{\parallel}}(k) &= \int \frac{d^3 k'}{(2\pi)^3} \left[\mu'^2 P_{\delta\delta}(|\mathbf{k} - \mathbf{k}'|) P_{vv}(k') \right. \\ &\quad \left. + \frac{(k - k' \mu') \mu'}{|\mathbf{k} - \mathbf{k}'|} P_{\delta v}(|\mathbf{k} - \mathbf{k}'|) P_{\delta v}(k') \right] \\ &+ \int \frac{d^3 k'}{(2\pi)^3} \frac{d^3 k''}{(2\pi)^3} \mu' \mu'' P_{\delta\delta vv}, \end{aligned} \quad (8)$$

where $\hat{\mathbf{k}} \cdot \hat{\mathbf{k}}' \equiv \mu'$, $\hat{\mathbf{k}} \cdot \hat{\mathbf{k}}'' \equiv \mu''$ and the arguments of the irreducible fourth moment $P_{\delta\delta vv}$ are the same as in Eq. (7). The term containing $P_{\delta\delta vv}$ is displayed here for

completeness; as we show below, it does not contribute significantly to either component at high k .

Perturbative Regime.—In the weak clustering regime, the full expressions in Eq. (8) can be simplified by using the linear relation $\tilde{\mathbf{v}} = \hat{\mathbf{k}} (\dot{a}f/k) \tilde{\delta}$, giving $P_{vv}^{(1)} = (f\dot{a}/k)^2 P_{\delta\delta}^{(1)}$ and $P_{\delta v}^{(1)} = (f\dot{a}/k) P_{\delta\delta}^{(1)}$, where $P_{\delta\delta}^{(1)}(k)$ is the power spectrum of the linear δ , \dot{a} is the expansion rate, and f is the familiar linear growth rate $f \approx \Omega_m^{-4/7}(z)$. The perturbative $P_{q_{\perp}}$ and $P_{q_{\parallel}}$ are then

$$\begin{aligned} P_{q_{\perp}}^{(2)}(k) &= \dot{a}^2 f^2 \int \frac{d^3 k'}{(2\pi)^3} P_{\delta\delta}^{(1)}(|\mathbf{k} - \mathbf{k}'|) P_{\delta\delta}^{(1)}(k') \\ &\quad \times \frac{k(k - 2k' \mu')(1 - \mu'^2)}{k'^2(k^2 + k'^2 - 2kk' \mu')}, \\ P_{q_{\parallel}}^{(2)}(k) &= \dot{a}^2 f^2 \int \frac{d^3 k'}{(2\pi)^3} P_{\delta\delta}^{(1)}(|\mathbf{k} - \mathbf{k}'|) P_{\delta\delta}^{(1)}(k') \\ &\quad \times \frac{k \mu' (k \mu' - 2k' \mu'^2 + k')}{k'^2(k^2 + k'^2 - 2kk' \mu')}. \end{aligned} \quad (9)$$

Note $\frac{1}{2} P_{q_{\perp}}^{(2)}$ here is the much studied OV term [5–11].

Nonlinear Regime.—Our main interest in this paper is the high- k , nonlinear behavior of P_q and its implications for the kinetic SZ effect. We obtain this by noting that the dominant contributions to the integrals in Eq. (8) are for \mathbf{k}' near the peak of $P_{\delta\delta}$ or P_{vv} . For high k beyond the peak, we can drop terms of $\mathcal{O}(k'/k)$ and obtain

$$P_{q_{\perp}}(k) = \frac{2}{3} \int \frac{d^3 k'}{(2\pi)^3} P_{\delta\delta}(k) P_{vv}(k') = 2P_{q_{\parallel}}(k). \quad (10)$$

The contribution from $\mathbf{k}' \approx \mathbf{k}$ is proportional to $P_{vv}(k)$ or $P_{v\delta}(k)$, which fall off much faster at large k . The fourth moment term is also negligible at all scales (see below). The result in Eq. (10) does not assume vanishing velocity-density cross correlation, but only that $P_{\delta\delta} P_{vv}$ and $P_{\delta v} P_{\delta v}$ are of similar order. The high- k result depends on the velocity power spectrum only through the integral $\int d^3 k' P_{vv}(k')/(2\pi)^3 = \langle v^2 \rangle$, the volume-averaged velocity dispersion, which is less sensitive to high- k nonlinear effect and appears only in the overall amplitude of $P_{q_{\perp}}$. Nonlinear contributions to the kinetic SZ effect therefore come mostly from $P_{\delta\delta}(k)$.

We compute the kinetic SZ power spectrum using the nonlinear halo model for $P_{\delta\delta}$ [14]. In this model, mass is assumed to be distributed in a collection of spherically symmetric halos with density profile $\rho(r)/\bar{\rho} = A u(r/r_s)$, where $u(x)$ is a specified function, and the density amplitude A and scale r_s are functions of halo mass. Moments of density are then superpositions over halo masses with given mass function dn/dM and halo-halo correlations. Statistics on small scales are dominated by contributions from particles in a single halo; for example, the nonlinear mass power spectrum is

$$P_{\delta\delta}(k) = \int dM \frac{dn}{dM} [A r_s^3 \tilde{u}(kr_s)]^2, \quad (11)$$

where $\tilde{u}(q)$ is the Fourier transform of $u(x)$. The halo model agrees well with numerical simulations for second and third moments of density and for pair velocity moments, and allows ab initio construction of and physical insight into a wide variety of density and velocity statistics [14]. In the halo model the contribution from the irreducible fourth moment to $P_{q\perp}$ vanishes since $P_{\delta\delta vv}$ has no dependence on ϕ', ϕ'' ; while its contribution to $P_{q\parallel}$, related by the equation of continuity to $\dot{\delta}$, is found to be negligible on all scales, falling as a high power of k for large k .

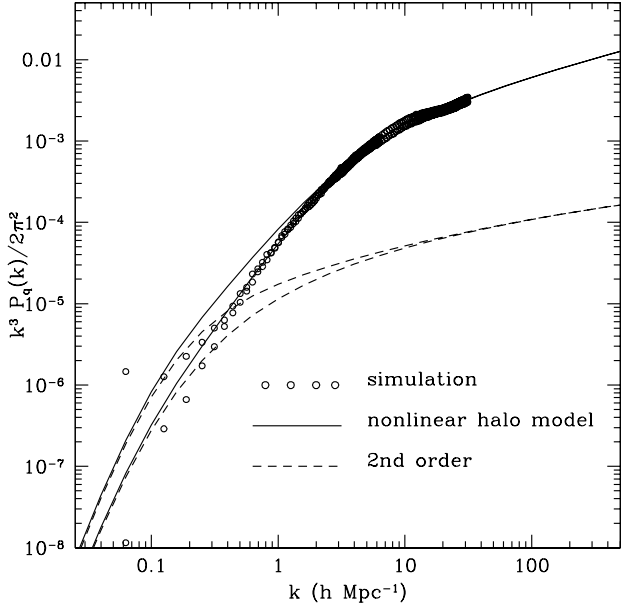


FIG. 1. 3-d Power spectrum of the density-weighted velocity $P_{q\parallel}$ (upper) and $\frac{1}{2}P_{q\perp}$ (lower). Our nonlinear analytical results (solid) agree well with simulations (open circle), whereas the second order OV approach (dashed) underestimates the high- k power by up to two orders of magnitudes. The model is CDM with matter density $\Omega_m = 0.3$, cosmological constant $\Omega_\Lambda = 0.7$, Hubble parameter $h = 0.75$, baryon density $\Omega_b = 0.05$, and COBE normalization $\sigma_8 = 0.92$ for rms density fluctuations on $8 h^{-1} \text{Mpc}$ scale.

Results.—Fig. 1 shows $P_{q\parallel}$ and $\frac{1}{2}P_{q\perp}$ for the density-weighted velocity \tilde{q} as obtained by three different methods: the second-order OV expression of Eq. (9); the nonlinear expression Eq. (10) evaluated in the halo model of Eq. (11); and numerical simulations. The simulation results (symbols) are computed directly from the particle positions and velocities in an output of a particle-particle particle-mesh N -body run with 128^3 particles in a $(100 \text{ Mpc})^3$ comoving box and a force resolution of 30 kpc. The halo model results (solid curves) are computed using the universal profile $u(x) = x^{-3/2}(1+x)^{-3/2}$ which approximates closely the dark matter halos found in high resolution N -body simulations [15]. A concentration parameter of $c(M, z) = r_{200}/r_c = 5(1 +$

$z)^{-1}[M/(5.5 \times 10^{14} M_\odot)]^{-1/6}$ is used for the ratio of the halo virial and core radii. Fig. 1 shows that the nonlinear contributions beyond second order in perturbation theory are important at $k > 1 \text{ Mpc}^{-1}$ and must be included for reliable calculations of the kinetic SZ effect. We also note that the nonlinear halo model is able to reproduce closely the high- k behavior of both $P_{q\parallel}$ and $P_{q\perp}$ in the simulation. Moreover, the simulation supports that $P_{q\parallel} = \frac{1}{2}P_{q\perp}$ on small scales and verifies that the contribution from the fourth moment $P_{\delta\delta vv}$ is unimportant on all scales. Fig. 1 illustrates the validity and the importance of our nonlinear treatment.

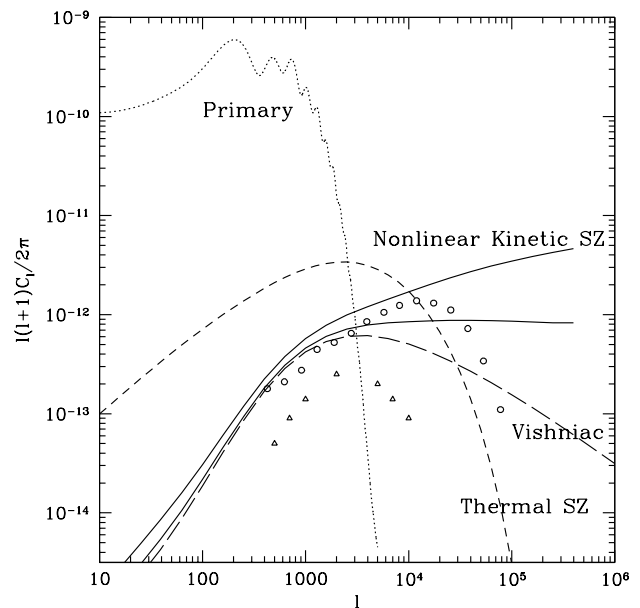


FIG. 2. Angular power spectrum for the kinetic SZ effect calculated from the nonlinear halo model assuming electrons follow the universal dark matter profile (upper solid) and the $\beta = 2/3$ profile inferred from X-ray observations (lower solid). Second-order perturbation theory (long-dashed) underestimates C_ℓ at high ℓ . For comparison we also show results from the hydrodynamical simulations of Springel et al. (circles) and da Silva et al. (triangles), the thermal SZ spectrum in the halo model (short-dashed), and the primary CMB spectrum (dotted). The model is the same as in Fig. 1.

Fig. 2 shows our predictions for the angular power spectrum of temperature fluctuations due to the nonlinear kinetic SZ effect (solid), compared with the primary CMB spectrum (dotted), the second order OV effect (long-dashed), and the thermal SZ in the Raleigh-Jeans regime (short-dashed). Our nonlinear results are obtained from Eq. (4), integrating $P_{q\perp}(k, z)$ (shown at $z = 0$ in Fig. 1) out to a reionization redshift of $z_r = 20$. Not surprisingly, values of C_ℓ at large ℓ (small angular scale) from our nonlinear method are significantly higher than obtained from second-order perturbation theory. The specific predictions of the halo model vary with

the assumed density profile. The dark matter profile used in Fig. 1 leads to higher C_ℓ than for the β -profile $\rho_b(r)/\bar{\rho} = A [1 + (r/r_c)^2]^{-3\beta/2}$ with $\beta = 2/3$ (lower solid), which provides a reasonable overall fit to the hot gas in galaxies and clusters, due to the flat inner core of the latter. For the β -profile core radius we use $r_c = r_{200}/c$, with $c(M, z) = 15(1+z)^{-1}[M/(1.8 \times 10^{13} h^{-5/2} M_\odot)]^{-0.1}$ derived from ROSAT clusters [16].

Besides details of the baryon profile, the predicted C_ℓ depends on the epoch of reionization and the lower halo mass cutoff in Eq. (11). The amplitude of C_ℓ is increased for earlier reionization, or when more low-mass halos host hot baryons. Neither is well determined by current observations and theories, but they are easily parameterized in our analytic formulation. Our analytical prediction is in broad agreement with results from hydrodynamical simulations [12]. Differences at high ℓ are likely due to simulation resolution and assumed ionization history. A model of inhomogeneous reionization in a distribution of bubbles [17] shares many features of the halo model but differs in details such as halo profile shapes and in the end leads to predictions about a factor of 10 smaller. This is perhaps due to both the cosmological model and assumptions about the distribution of ionized matter.

Discussion.— We have derived analytical expressions for the nonlinear kinetic SZ effect on the CMB and computed the anisotropy power spectrum C_ℓ from the nonlinear power spectrum P_q of the density weighted velocity $\mathbf{q} = (1 + \delta)\mathbf{v}$ using the recently developed halo model of nonlinear clustering. All scales where the kinetic SZ effect is not overwhelmed by the primary CMB anisotropy are in the regime of strongly nonlinear clustering, where the second-order OV calculation underestimates the result and a fully nonlinear formulation is essential.

We have studied both the transverse and longitudinal components of \mathbf{q} and found that $P_{q_\perp} \approx 2P_{q_\parallel}$ at high k . Although only $\tilde{\mathbf{q}}_\perp$ contributes to the kinetic SZ effect, we note that $\tilde{\mathbf{q}}_\parallel$ is directly proportional to the rate of growth of the density field, so a realistic nonlinear model for δ can in principle be used to compute the nonlinear kinetic SZ effect. We find both analytically and in simulations that a potential contribution from a density-velocity irreducible fourth moment does not make an appreciable contribution to either P_{q_\perp} or P_{q_\parallel} . In the halo model, it is easy to see that in the integrated kinetic SZ effect contributions entering and exiting a single, spherically symmetric halo precisely cancel; the observed effect depends on the additional motions of halo centers. Contributions from rotational flow velocities or non-spherical halos may change geometric factors and alter these conclusions in detail, but the main features should remain the same.

An earlier attempt [11] to include effects of nonlinearity started with the second order OV expression (9), replaced the density power spectrum with a nonlinear form, left the linear velocity power unchanged but filtered on a

scale k_F , argued that density-velocity cross-correlations are unimportant, and retained the mode couplings that were derived in perturbation theory. The OV expression actually includes contributions from density-velocity cross correlations, which with the linear density-velocity relation enter at the same order. At large k , however, the contribution from the cross-correlation term is negligible after integration over angle, as we found in obtaining Eq. (10); the perturbative expression therefore also reduces to (10). This result then depends on the poorly known velocity spectrum P_{vv} only through its integral over all k , or the velocity dispersion $\langle v^2 \rangle$, which appears only as an overall normalization factor and is less sensitive to the high- k nonlinear effects. Our fully nonlinear formulation therefore indicates that the nonlinearity in kinetic SZ effect comes mostly from the density power spectrum.

We have enjoyed discussions with Ed Bertschinger, Bhuvnesh Jain, Ue-Li Pen, Max Tegmark, and Martin White. C.-P. M. acknowledges support of an Alfred P. Sloan Foundation Fellowship, a Cottrell Scholars Award from the Research Corporation, a Penn Research Foundation Award, and NSF grant AST 99-73461.

- [1] Y. B. Zeldovich and R. A. Sunyaev, *Astron. Astrophys.*, 20, 189 (1969); for a recent review see M. Birkinshaw, *Physics Reports*, 310, 97 (1999).
- [2] R. A. Sunyaev, *Sov. Astron. Lett.*, 3, 491 (1977).
- [3] N. Kaiser, *ApJ*, 282, 374 (1984).
- [4] J. P. Ostriker and E. T. Vishniac, *ApJ*, 306, L51 (1986).
- [5] E. T. Vishniac, *Astrophys. J.*, 322, 597 (1987).
- [6] G. Efstathiou, in *Large-Scale Motions*, ed. V. Rubin and S. J. Coyne (Princeton University Press, Princeton, 1988), p. 299.
- [7] S. Dodelson and J. M. Jubas, *ApJ*, 439, 503 (1993).
- [8] W. Hu, D. Scott, and J. Silk, *Phys. Rev. D* 49, 648 (1994).
- [9] W. Hu and M. White, *Astron. Astrophys.*, 315, 33 (1996).
- [10] A. H. Jaffe and M. Kamionkowski, *Phys. Rev. D* 58, 043001 (1998).
- [11] W. Hu, *ApJ*, 529, 12 (2000).
- [12] V. Springel, M. White, and L. Hernquist, *ApJ*, 549, 681 (2001); A. C. da Silva et al., *MNRAS*, 317, 37 (2001); N. Y. Gnedin and A. H. Jaffe, *ApJ*, 551, 3 (2001).
- [13] N. Kaiser, *ApJ*, 388, 272 (1992).
- [14] C.-P. Ma and J. N. Fry, *ApJ*, 543, 503 (2000); C.-P. Ma and J. N. Fry, *ApJ*, 538, L107 (2000); U. Seljak, *MNRAS*, 318, 203 (2000); and references therein.
- [15] B. Moore, et al., *MNRAS*, 310, 1147 (1999).
- [16] J. Mohr, B. Mathiesen & A. Evrard, *ApJ*, 517, 627 (1999).
- [17] P. Valageas, A. Balbi & J. Silk, *A&A*, 367, 1 (2001).